

Does the Potential Vorticity Distribution Constrain the Spreading of Floats in the North Atlantic?

JANE O'DWYER

Norwegian Polar Institute, Tromsø, Norway

RICHARD G. WILLIAMS

Oceanography Laboratories, University of Liverpool, Liverpool, United Kingdom

JOSEPH H. LACASCE

Woods Hole Oceanographic Institution, Woods Hole, Massachusetts

KEVIN G. SPEER

Laboratoire de Physique des Océans, IFREMER/CNRS, Plouzane, France

(Manuscript received 21 August 1998, in final form 2 June 1999)

ABSTRACT

Float trajectories are compared with the distribution of climatological potential vorticity, Q , on approximate isentropic surfaces for intermediate waters in the North Atlantic. The time-mean displacement and eddy dispersion are calculated for clusters of floats in terms of their movement along and across Q contours. For float clusters with significant mean velocities, the mean flow crosses Q contours at an angle of typically less than 20° – 30° in magnitude in the ocean interior. The implied Peclet number in the ocean interior ranges from 1 to 19 with a weighted-mean value of 4.4. This mean Peclet number suggests that there is significant eddy mixing in the ocean interior: tracers should only be quasi-conserved along mean streamlines over a subbasin scale, rather than over an entire basin. The mean flow also strongly crosses Q contours near the western boundary in the Tropics, where the implied Peclet number is 0.7; this value may be a lower bound as Q contours are assumed to be zonal and relative vorticity is ignored. Float clusters with a lifetime greater than 200 days show anisotropic dispersion with greater dispersion along Q contours, than across them; float clusters with shorter lifetimes are ambiguous. This anisotropic dispersion along Q contours cannot generally be distinguished from enhanced dispersion along latitude circles since Q contours are generally zonal for these cases. However, for the null case of uniform Q for the Gulf Stream at 2000 m, there is strong isotropic dispersion, rather than enhanced zonal dispersion. In summary, diagnostics suggest that floats preferentially spread along Q contours over a subbasin scale and imply that passive tracers should likewise preferentially spread along Q contours in the ocean interior.

1. Introduction

Float trajectories provide a Lagrangian measure of the circulation, which is usually interpreted in terms of zonal and meridional displacements; see studies by Freeland et al. (1975) and Krauss and Böning (1987). Here, we argue that the movement of floats may be viewed more naturally in terms of their spreading along and across potential vorticity contours. The large-scale potential vorticity (neglecting relative vorticity) is defined by

$$Q = -\frac{f}{\rho_0} \frac{\partial \sigma}{\partial z},$$

where f is the planetary vorticity, ρ_0 is a reference density, and $\partial \sigma / \partial z$ is the vertical gradient of locally referenced potential density.

The rate of change of Q of a fluid parcel moving with velocity \mathbf{u} and experiencing a forcing \mathcal{F} is

$$\frac{DQ}{Dt} = \frac{\partial Q}{\partial t} + \mathbf{u} \cdot \nabla Q = \mathcal{F}, \quad (1)$$

and a time and space average of (1) gives

$$\frac{\partial \overline{Q}}{\partial t} + \overline{\mathbf{u}} \cdot \nabla \overline{Q} = \overline{\mathcal{F}} - \nabla \cdot \overline{\mathbf{u}'Q'}, \quad (2)$$

Corresponding author address: Dr. J. O'Dwyer, Norsk Polarinstitutt, Polarmiljøsenenteret, N-9296 Tromsø, Norway.
E-mail: jane@npolar.no

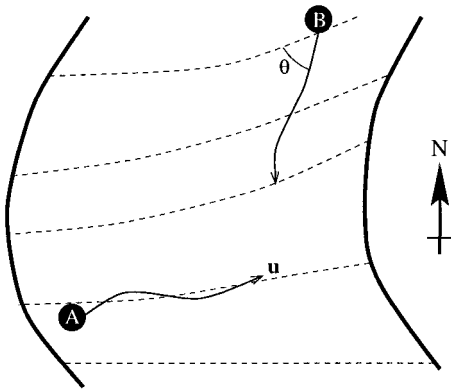


FIG. 1. On an isentropic surface, a trajectory makes an angle θ with Q (dashed contours) implying a Peclet number $Pe = 1/\tan\theta$. Fluid parcel A, in the free limit, moves nearly parallel to Q contours with $DQ/Dt \approx 0$ and Pe is large. By contrast in the forced or diffusive limit, where $DQ/Dt \neq 0$, fluid parcel B crosses Q contours with large θ and Pe is small.

where the overbars indicate means evaluated over time and space and primes indicate eddy fluctuations.

According to (1) the instantaneous motion of fluid parcels tends to conserve Q , with a deviation depending on \mathcal{F} . In the time- and spatially averaged case (2), fluid parcels cross the time-mean, large-scale \bar{Q} contours due to the mean forcing and the divergence of eddy fluxes. Different limits are illustrated in Fig. 1. In the unforced limit (trajectory A) flow follows Q contours, and in the forced limit (trajectory B) flow crosses Q contours. The extent to which a fluid parcel crosses Q contours is measured by the angle θ between the trajectory and the contours. The angle θ is a measure of the effect of advection compared with the combined effects of diffusion and forcing, and following Rhines and Schopp (1991), θ can be related to the Peclet number:

$$Pe = \frac{|\bar{\mathbf{u}} \times \nabla \bar{Q}|}{\bar{\mathbf{u}} \cdot \nabla \bar{Q}} = \frac{1}{\tan\theta}, \quad (3)$$

where $\bar{\mathbf{u}} \cos\theta$ and $\bar{\mathbf{u}} \sin\theta$ measure the mean velocity component parallel and normal to the Q contours; this ratio is equivalent to the ratio of the vector cross product and scalar product of the velocity vector with ∇Q . This Peclet number differs from the traditional definition, $Pe = UL/\kappa$, in avoiding the ambiguous choice of a characteristic length scale L ; U is a velocity scale and κ is the diffusivity. In the following float diagnostics, we evaluate the mean angle with which floats move relative to the Q contours and hence estimate the Peclet number.

Float diagnostics from a collection of experiments are compared with Q inferred from climatology for intermediate waters in the North Atlantic. This study complements the comparison of isothermal floats with synoptic Q in the Subduction Experiment (Price and Owens 1998), the recent float study examining the crossover of the Gulf Stream and deep western boundary current (Bower and Hunt 2000) and the comparison of float

trajectories with f/H (where H is full the ocean depth) by LaCasce and Speer (1999). The datasets are described in section 2. Mean and eddy components of the flow are evaluated in terms of Q coordinates in sections 3 and 4, respectively. In section 5 we summarize our results and discuss the implications for the distribution of passive tracers.

2. Potential vorticity and float data

a. Climatological potential vorticity

The Q distribution is evaluated using bottle data from the National Oceanographic Data Center; see Levitus and Boyer (1994) and Levitus et al. (1994) for a description of the temperature and salinity data. We perform our analysis on surfaces that approximate the isentropic surfaces followed by fluid parcels in the absence of diapycnal mixing; this approach avoids isobaric smoothing, which can distort water mass properties (Lozier et al. 1994). Here Q is evaluated from the vertical spacing of the isentropic surfaces,

$$Q = -\frac{f}{(1000 + \gamma^n) \Delta z},$$

where z is the depth of the neutral surface, labeled γ^n , calculated using the algorithm of Jackett and McDougall (1997), and Δz is the vertical spacing of the surfaces $\gamma^n \pm \frac{1}{2}\Delta\gamma^n$.

For each set of floats, Q is interpolated onto a one-degree grid along the approximate isentropic surface, γ^n , close to the depth of the floats (see Table 1); see O'Dwyer and Williams (1997) for a more detailed description of the procedure. The standard error is typically less than 10% of the Q signal over most of the ocean interior. The resulting Q distribution is a time average, but for the sake of simplicity we omit the overbar from Q .

b. Neutrally buoyant floats

The float trajectories are taken from experiments conducted in the intermediate waters of the tropical and North Atlantic, listed in Table 1. The trajectories include historical data from the tropical Atlantic, the western North Atlantic and the eastern North Atlantic at depths between 700 and 2000 m and the first two years of data from the Eurofloat study in the eastern North Atlantic at 1750 m. Shallow floats within the seasonal boundary layer are excluded from this study: both because there is strong diabatic forcing within the seasonal boundary layer and because the seasonal variation of stratification will bias the mean Q distribution. Also excluded from this study are the floats deployed in meddies in the eastern Atlantic. The effect of these floats is discussed in section 3b.

We are interested in float trajectories as a proxy for the movement of water masses, which preferentially

TABLE 1. The float experiments used for the analysis, subdivided into northern and southern groups (labeled N and S). The γ^n surfaces were chosen to be at the appropriate depth in the region of each float experiment.

Experiment (reference)	Year	Position	Depth (m)	Number of floats	Float days, N	γ^n surface	Map	Label
PreLDE (Riser and Rossby 1983)	1976–79	25°–35°N, 40°–80°W	700	43	7552	27.50	Fig. 2a	PL (N)
		15°–25°N, 40°–80°W						PL (S)
Site L (Price et al. 1987)	1982–84	35°–40°N, 60°–80°W	700	33	5622	27.50	Fig. 2a	SL (N)
		30°–35°N, 60°–80°W						SL (S)
Gulf Stream recirculation (Owens 1991)	1980–85	35°–45°N, 40°–70°W	700	27	5374	27.50	Fig. 2b	GU (N)
		25°–35°N, 40°–70°W	2000	38	10 310	27.97	Fig. 2f	GU (S)
		30°–45°N, 40°–80°W						GU
Tropical Atlantic (Richardson et al. 1994)	1989–92	0°–10°N, 15°–60°W	800	18	7796	27.50	Fig. 2b	TA (N)
		–10°–0°N, 15°–60°W	1800	18	9798	27.95	Fig. 2d	TA (S)
		2°–10°N, 10°–60°W						TA (N)
		–5°–2°N, 10°–60°W						TA (S)
Eastern Basin (Zemanovich et al. 1990)	1984–91	30°–40°N, 15°–40°W	1100	38	21 337	27.70	Fig. 2c	EB (N)
		20°–30°N, 15°–40°W						EB (S)
Eurofloat (Speer et al. 1999)	1997–98	50°–60°N, 10°–40°W	1750	20	9163	27.95	Fig. 2e	EF (N)
		40°–50°N, 10°–40°W						EF (S)

spread along isentropic surfaces. Since floats are designed to follow isobaric surfaces, they are not strictly Lagrangian tracers (Davis 1991). In most regions of the North Atlantic, the isentropic surfaces are relatively flat, and Q diagnosed along level and isentropic surfaces is similar. However, there may be significant differences in the Gulf Stream region where there are strong flows and large horizontal density gradients.

c. Maps of Q and float trajectories

The trajectories for each float experiment are plotted on the maps of Q for the appropriate γ^n surface (Fig. 2). Near the equator Q contours are zonal on all the γ^n surfaces. Elsewhere the Q distribution varies with the surface. On the less dense surfaces, Q contours fan out from the southwest to the northeast (see $\gamma^n = 27.50$ and 27.70 in Figs. 2a,c). On denser surfaces, there is a Q maximum along the eastern boundary leading to meridional contours on $\gamma^n = 27.95$ and 27.97 (Figs. 2d,f). Along the Gulf Stream, there is a strong Q gradient on the less dense surfaces, but Q becomes nearly uniform on $\gamma^n = 27.97$ (Fig. 2f). This uniform Q signal has previously been diagnosed by McDowell et al. (1982) and O'Dwyer and Williams (1997) in the thermocline and deep waters, respectively. The groups of floats have been released in regions with nearly zonal Q contours, with two exceptions: the Eurofloat floats at 1750 m in the northeast Atlantic, where Q contours are nearly meridional (Fig. 2e), and the Gulf Stream at 2000 m, where Q is nearly uniform (Fig. 2f).

The float trajectories reveal two distinct regimes in the tropical Atlantic (Figs. 2b,d). In the interior, float trajectories at both 800 m and 1800 m have large zonal excursions along the zonal Q contours. Near the western boundary in the Tropics, float trajectories have a strong meridional component.

d. Defining Q coordinates

In the following sections, float displacements are analyzed in terms of a coordinate system aligned along and across Q contours (rather than along lines of longitude, x , and latitude, y). The coordinates are orientated according to the average ∇Q over each float group (so variations in the Q gradient over the group are ignored). This simplification appears reasonable given the relatively limited extent of each float group (Fig. 2); note that a variable angle for f/H is used by LaCasce and Speer (1999). The angle α is defined to measure the rotation of the Q coordinates with respect to x as shown in Fig. 3.

The mean angle, α , for each group of floats is evaluated from the sum of the individual angles, $\alpha_i(t)$ experienced by each float over time,

$$\alpha = \frac{1}{N} \sum \alpha_i(t).$$

The individual angle for each float position $\mathbf{x}_i(t)$ is given by

$$\alpha_i(t) = -\tan^{-1} \frac{\partial Q / \partial x_i(t)}{\partial Q / \partial y_i(t)},$$

where i labels a float and t is the time along the trajectory; the lateral Q gradients, $\partial Q / \partial x_i(t)$ and $\partial Q / \partial y_i(t)$, are calculated along the γ^n surface by bilinear interpolation of the one-degree gridded fields.

The mean angle of the Q contours experienced by the groups of floats is generally small, $|\alpha| < 25^\circ$ (Table 2). An exception is the southern Eurofloat site, where Q contours are nearly meridional, $\alpha \sim 70^\circ$, and there is a large variability arising from the high curvature of Q . In the Gulf Stream at 2000 m, Q is nearly uniform (Table 2) and it is not possible to determine α with any confidence; hence these floats are analyzed in terms of x

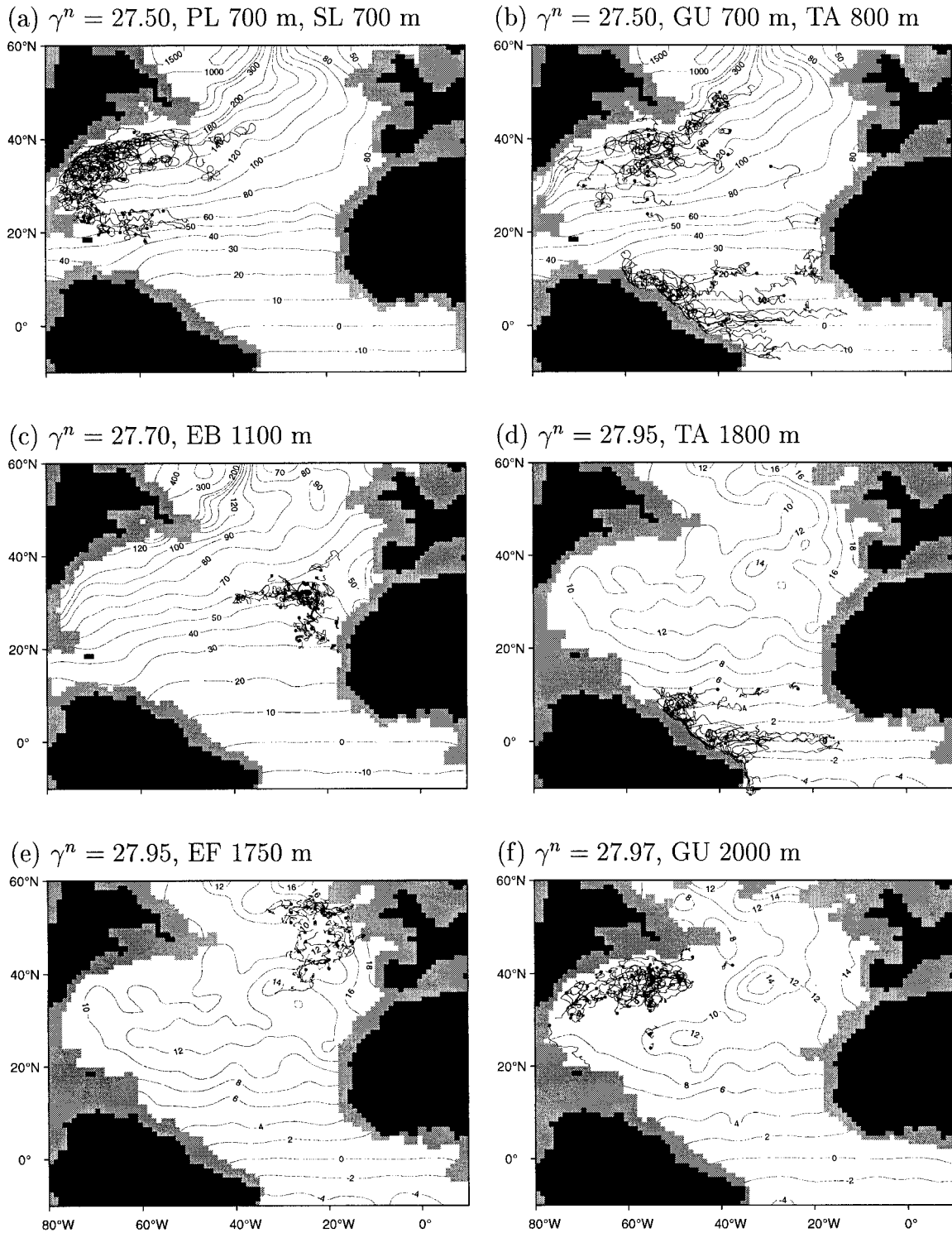


FIG. 2. Maps of float trajectories superimposed on the climatological Q ($10^{-12} \text{ m}^{-1} \text{ s}^{-1}$) for the appropriate γ^n surface: (a) Q on $\gamma^n = 27.50$ and float trajectories from PreLDE and SiteL at 700 m, (b) Q on $\gamma^n = 27.50$ and float trajectories from the Gulf Stream at 700 m and the tropical Atlantic at 800 m, (c) Q on $\gamma^n = 27.70$ and float trajectories from the Eastern Basin at 1100 m, (d) Q on $\gamma^n = 27.95$ and float trajectories from the tropical Atlantic at 1800 m, (e) Q on $\gamma^n = 27.95$ and float trajectories from Eurofloat at 1750 m, and (f) Q on $\gamma^n = 27.97$ and float trajectories from the Gulf Stream at 2000 m.

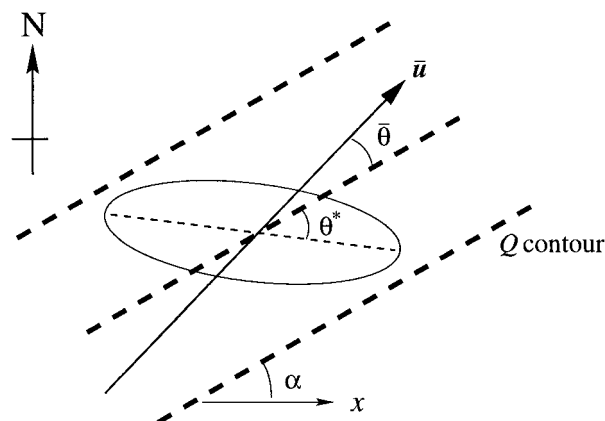


FIG. 3. Q contours (dashed lines) on an isentropic surface. The angle between Q contours and the x coordinate is measured by α . The mean velocity vector makes an angle $\bar{\theta}$ with Q contours, and the dispersion of a cluster of floats is shown by the ellipse with maximum dispersion at an angle θ^* to the Q contours.

and y displacements. Float trajectories are now analyzed in terms of their mean and eddy displacements along and across Q contours.

3. Analysis of mean float displacement

a. Evaluating mean velocity

The time-mean Eulerian velocity is evaluated over specified regions (defined in Table 1) from the float velocities

$$\bar{\mathbf{u}} = \frac{1}{N} \sum \mathbf{u}_i(t), \quad (4)$$

where $\mathbf{u}_i(t)$ is the daily float velocity calculated from the float positions and the summation is applied for all time and every float within the specified region. Note that this Eulerian estimate differs from a Lagrangian

estimate, which would include contributions when floats move outside the specified region; see Davis (1991) for more discussion of this issue.

In our analysis, the partitioning of the “mean” and “eddy” signatures depends partly on the size of the region over which the float data are binned. Defining smaller regions provides more information about spatial variations in the mean velocity, but the errors become larger due to the reduced numbers of floats. Conversely, defining larger regions leads to more statistically significant flows, but leads to small-scale, time-mean flow being aliased into the “eddy” statistics. Here we choose to divide each float experiment into a northern and southern group. The mean flow is evaluated for each group, and eddy dispersion is evaluated whenever there are more than 10 floats with trajectories longer than 100 days. Float trajectories in the tropical Atlantic are further separated into the interior, where the climatological Q field is evaluated, and in a boundary region, where Q is not calculated from climatology but assumed to be zonal, as is observed in the interior.

The time-mean Eulerian velocities, evaluated from floats within each region, range in magnitude between 0.3 mm s^{-1} and 81 mm s^{-1} (Table 3). The root-mean-square eddy velocity, u_e (the standard deviation) is typically an order of magnitude larger than the mean and is nearly isotropic; further details are given in section 4a. In general, both the mean and eddy velocities decrease with depth. Floats at 700 m and 800 m are more energetic than deeper floats. In many cases the standard error is comparable to the mean velocity.

b. Interior mean flow

The mean flow in the interior is generally greater along Q contours than across them, as shown in Table 3. This result holds for all statistically significant flows (boldfaced in Table 3). For the southern Eastern Basin

TABLE 2. For each float group, the Q field is characterized by \bar{Q} , $\overline{|\nabla Q|}$, and α , the angle Q contours cross latitude circles. The standard deviation of α gives an indication of how uniform the direction of Q contours is over the region occupied by the floats.

Experiment	Depth (m)	\bar{Q} ($10^{-12} \text{m}^{-1} \text{s}^{-1}$)	$\overline{ \nabla Q }$ ($10^{-18} \text{m}^{-2} \text{s}^{-1}$)	Angle α (deg)
PreLDE (N)	700	123	80	25 (± 8)
PreLDE (S)	700	67	52	14 (± 1)
Site L (N)	700	183	140	17 (± 3)
Site L (S)	700	149	96	21 (± 12)
Gulf Stream (N)	700	171	122	21 (± 6)
Gulf Stream (S)	700	119	60	10 (± 2)
Gulf Stream	2000	8	1	—
Tropical Atlantic (N)	800	9	15	4 (± 1)
Tropical Atlantic (S)	800	-7	15	2 (± 1)
Tropical Atlantic (N)	1800	4	4	2 (± 1)
Tropical Atlantic (S)	1800	0	5	2 (± 1)
Eastern Basin (N)	1100	53	21	15 (± 1)
Eastern Basin (S)	1100	42	19	13 (± 2)
Eurofloat (N)	1750	12	9	-22 (± 36)
Eurofloat (S)	1750	13	7	70 (± 27)

TABLE 3. Mean and eddy velocities of each group of floats evaluated along and across Q contours. Note how the mean velocity is greater along the Q contours than across them, whereas the eddy velocity is nearly isotropic. The tropical Atlantic float trajectories are separated into those in the interior and the boundary current. Standard errors are shown in brackets and velocities significantly different from zero are bold font. θ is the angle between the mean velocity and Q contours, and $Pe = 1/\tan \theta$ is an estimate of the implied Peclet number. The asterisks (3) in the depth column indicate velocities in terms of x - y rather than Q coordinates.

Experiment	Depth (m)	Mean velocity (10^{-3}m s^{-1})			Pe	Eddy velocity (10^{-3}m s^{-1})	
		Along Q	Across Q	$\bar{\theta}(\circ)$		Along Q	Across Q
			Interior flow				
PreLDE (N)	700	-11.4 (± 4.3)	5.5 (± 4.4)	-25	2.1	76 (± 6)	78 (± 6)
PreLDE (S)	700	6.1 (± 3.0)	-4.8 (± 3.0)	-38	1.3	62 (± 4)	62 (± 4)
Site L (N)	700	81.1 (± 17.4)	-4.6 (± 15.2)	-3	19.1	240 (± 24)	211 (± 21)
Site L (S)	700	-29.9 (± 6.0)	3.3 (± 5.9)	-6	9.5	116 (± 8)	114 (± 8)
Gulf Stream (N)	700	15.4 (± 10.0)	3.5 (± 9.6)	13	4.3	157 (± 14)	152 (± 13)
Gulf Stream (S)	700	0.3 (± 4.9)	-3.1 (± 4.9)	-85	0.1	123 (± 5)	119 (± 5)
Gulf Stream	2000 *	-2.7 (± 2.3)	1.1 (± 2.4)	—	—	74 (± 3)	75 (± 3)
Tropical Atlantic (N)	800	5.6 (± 3.6)	-2.1 (± 2.9)	-20	2.7	91 (± 5)	72 (± 4)
Tropical Atlantic (S)	800	30.7 (± 8.2)	-9.0 (± 5.4)	-16	3.5	96 (± 11)	63 (± 7)
Tropical Atlantic (N)	1800	0.5 (± 2.6)	0.8 (± 2.8)	56	0.7	55 (± 4)	59 (± 4)
Tropical Atlantic (S)	1800	3.3 (± 3.2)	1.2 (± 2.0)	20	2.7	73 (± 4)	45 (± 3)
Eastern Basin (N)	1100	-3.2 (± 0.8)	-0.7 (± 0.9)	12	4.7	38 (± 1)	39 (± 1)
Eastern Basin (S)	1100	0.8 (± 1.0)	-0.1 (± 1.2)	-8	7.4	22 (± 2)	27 (± 2)
EB(S) with meddies	1100	-0.3 (± 1.3)	-2.6 (± 1.4)	83	0.1	38 (± 2)	40 (± 2)
Eurofloat (N)	1750	-3.8 (± 2.4)	2.6 (± 2.5)	35	1.4	45 (± 3)	47 (± 3)
Eurofloat (S)	1750	-6.5 (± 1.3)	1.0 (± 1.2)	-9	6.3	31 (± 2)	30 (± 2)
			Boundary flow				
Tropical Atlantic	800 *	-12.7 (± 8.8)	17.1 (± 8.9)	-54	0.7	97 (± 12)	98 (± 12)
	1800 *	14.8 (± 19.3)	-20.5 (± 17.2)	-53	0.7	107 (± 27)	96 (± 24)

group the floats deployed in meddies have been excluded from the analysis [see the example in Richardson et al. (1989)]. These floats strongly cross Q contours and imply that the mean flow crosses Q contours at an angle of 83° compared to -8° without them. This signal is consistent with theoretical studies suggesting that meddies are intense, isolated vortices, which are prone to drift across mean potential vorticity contours (Flierl 1987; Colin de Verdiere 1992).

The mean flow also apparently crosses Q contours with a large angle in the southern group for the Gulf Stream and the northern group for the tropical Atlantic at 1800 m, but these angles are unreliable since the velocities are small and not significantly different from zero. In the case of nearly uniform Q for the Gulf Stream floats at 2000 m, the mean flow is stronger in the zonal direction, but again the standard error is large compared with the mean.

In most cases, the alignment of the mean flow with Q contours is equivalent to greater zonal than meridional flow, since the Q contours are nearly zonal. However, in the southern Eurofloat region, Q contours and the mean velocity are both nearly meridional; Q contours are at an angle of 70° to latitude circles and the mean flow only differs from Q contours by -9° .

These comparisons ignore the contribution of relative vorticity, ζ , to the potential vorticity. While ζ is small compared with the planetary vorticity, f , their gradients become comparable on eddy scales. For example, a typical eddy velocity of 10 cm s^{-1} and a length scale of 100 km implies $\zeta \sim 10^{-6}\text{ s}^{-1}$, which is smaller than f

except close to the equator. However, the ratio of the gradients, $\nabla\zeta/\beta \sim U/(\beta L^2) \sim 1$, for a horizontal scale $L \sim 100\text{ km}$ and the planetary vorticity gradient $\beta \sim 10^{-11}\text{ m}^{-1}\text{ s}^{-1}$. Therefore, these comparisons are probably only robust when the floats have spread over a scale greater than the eddy deformation scale.

c. Interior Peclet number

The angle of the floats to the Q contours implies a Peclet number (3) ranging from typically 1 to 19 in the interior (Fig. 4). Floats trapped in meddies in the southern Eastern Basin group behave anomalously, strongly crossing Q contours. The Peclet number here has a typical value of 7.4 when the meddies are excluded, but the Peclet number decreases to 0.1 if floats within meddies are included in the analysis (Table 3). There is also a low Peclet number of 0.1 for the southern group in the Gulf Stream, but this estimate is unreliable since the velocities are not statistically significant.

The mean Peclet number is 4.4 for all the floats weighted by the number of float days (excluding those trapped in meddies), which implies that there is significant mixing in the ocean interior. This Peclet number is comparable to values from 3 to 6 diagnosed in eddy-resolving numerical experiments (Rhines and Schopp 1991), but is much lower than the high Peclet number implied by ideal thermocline models. In comparison, Jenkins (1988) has diagnosed a relatively low Peclet number between 1 and 2 from observations of tritium-helium age, and Robbins et al. (2000) infer a Peclet

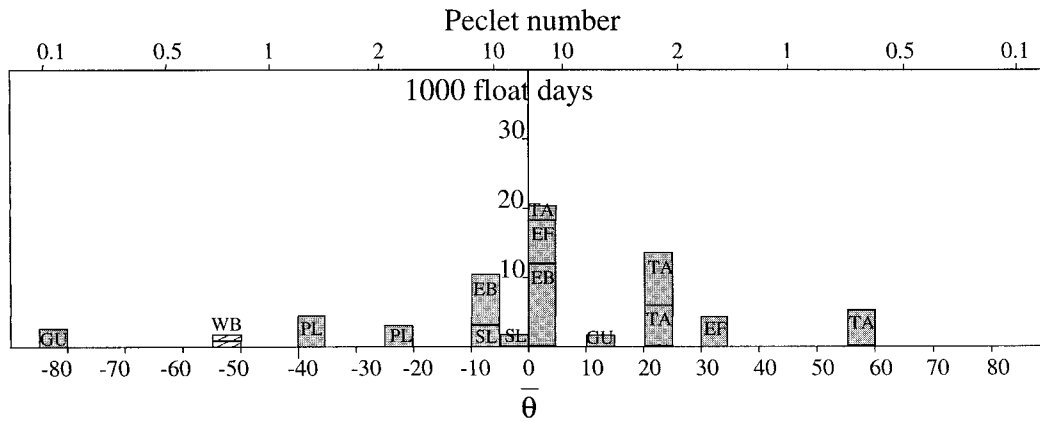


FIG. 4. Histogram of $\bar{\theta}$, the angle between the mean flow and the Q contours. Boxes are labeled according to Table 1. The size of a box indicates the number of observations used in the analysis; boxes labeled WB are the tropical western boundary floats. The implied Peclet number, $Pe = 1/|\tan\bar{\theta}|$, is also indicated and has a weighted-mean value of 4.4 over the ocean interior.

number decreasing from 13 to 1.7 along $\sigma = 26.5$ and $\sigma = 27.1$ surfaces, respectively, in the eastern North Atlantic.

While the low Peclet number implies that there is mixing on a subbasin scale, there is no conclusive pattern of up- or downgradient movement of the floats, as found by comparing $\bar{\mathbf{u}} \cdot \nabla Q$ and $\nabla^2 Q$. The lack of this signal may partly be due to the cross- Q flow often being smaller than the standard errors (Table 3).

The Peclet number can be used to estimate the length scale over which tracer contrasts advected into the ocean are likely to persist (Fig. 5). For example, consider a tracer contrast with an initial horizontal scale L_{tracer} . As the tracer moves downstream, the initial contrast will be smeared out over a scale $L_{\text{signal}} = L_{\text{tracer}}/\tan\theta = L_{\text{tracer}}Pe$. Therefore, if tracer contrasts are injected into the domain across streamlines over a lateral scale of $L_{\text{tracer}} \sim 300$ km, then the Peclet number estimate of typically 4 in the interior implies that the signal will persist downstream for 1200 km along mean streamlines before being smeared out. Therefore we expect that trac-

ers should be quasi-conserved on the subbasin scale, rather than over an entire basin.

d. Mean flow in the tropical western boundary

The time-mean flow in the western boundary in the Tropics is aligned with the coastline. If the Q contours are assumed to remain zonal in the boundary, then there is a strong cross- Q flow implying vigorous mixing and dissipation; note that Q is not defined in the shaded regions in Fig. 2. The implied Peclet number reaches low values of 0.7 for both the floats at 800 m and 1800 m (Fig. 4). However, this estimate may reflect a lower bound since Q contours might instead be advected along the topography and relative vorticity gradients may become significant.

In summary, two different regimes are revealed here: an interior regime where floats weakly cross Q contours, with a Peclet number of typically 4, and a boundary regime where floats strongly cross Q contours, with a Peclet number less than 1. We now examine whether the Q distribution constrains the dispersion of clusters of floats relative to their center of mass.

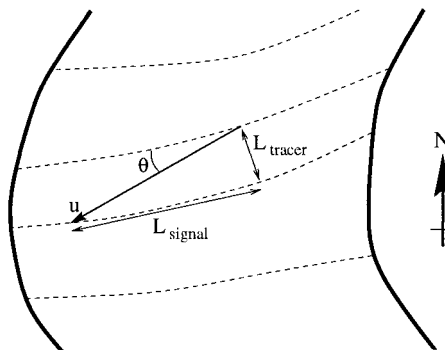


FIG. 5. The relationship between the tracer distribution (dashed contours), mean velocity (vector labeled \mathbf{u}), and Peclet number ($1/\tan\bar{\theta}$).

4. Analysis of eddy dispersion

a. Evaluating eddy velocities and dispersion

Each float trajectory is separated into a contribution from the time-mean Eulerian velocity over a particular region (defined in Table 1) and an eddy deviation,

$$\mathbf{x}_i(t) = \bar{\mathbf{x}}(t) + \mathbf{x}'_i(t), \quad \mathbf{u}_i(t) = \bar{\mathbf{u}} + \mathbf{u}'_i(t),$$

where \mathbf{x}' and \mathbf{u}' are the eddy displacement and eddy velocity, which include contributions from both the temporal and spatial variations in the flow; $\bar{\mathbf{x}}(t) = \bar{\mathbf{u}}t$ is the mean displacement from the original position and $\bar{\mathbf{u}}$ is the mean velocity for that particular region (4).

The eddy velocity is typically an order of magnitude larger than the mean velocity. The estimated errors in eddy velocity are only a factor of $1.96/\sqrt{2}$ larger than the error for the mean velocity; therefore the percentage error is much smaller for the eddy velocity than for the mean velocity.

For a particular direction the eddy dispersion $x_e(t)$ at a time t and the root-mean-square eddy velocity, u_e , are given by the standard deviations:

$$x_e(t) = \left[\frac{1}{N} \sum_i x_i'(t)^2 \right]^{1/2} \quad u_e = \left[\frac{1}{N} \sum \mathbf{u}_i'(t)^2 \right]^{1/2}.$$

Assuming a Gaussian distribution, the 95% confidence limits for each quantity are given by the factor $(1 \pm 1.96/\sqrt{2n})$, where $n = N/(T \times \text{frequency of observation})$ is an estimate of the number of independent observations and T is the Lagrangian timescale, assumed a priori to have a value of $T = 10$ days.

We now analyze how the floats disperse away from the center of mass for each float cluster, both along x and y and along and across Q contours. Since we expect the effect of the Q field only to be apparent on timescales longer than that for an individual geostrophic eddy, we focus on the float groups containing more than 10 floats with records longer than 100 days.

b. Eddy dispersion in the interior

The dispersion increases with time for each group of floats, as shown in Fig. 6. For float groups with long records, the dispersion is greater along Q than across Q (see Fig. 7 and Table 4), as shown in the tropical Atlantic and Eastern Basin (compare the thick full and dashed lines in Fig. 6). For these cases, the ratio of the eddy dispersion along Q to across Q is close to the ellipticity of the eddy dispersion ellipse (see Table 4 and the ellipses plotted in Fig. 8). Float groups with shorter lifetimes are ambiguous: PreLDE shows greater dispersion along Q , whereas Site L shows less dispersion, and the southern Eurofloat group appears to be isotropic.

When there is anisotropy, the enhanced dispersion along Q is consistent with enhanced zonal dispersion since Q contours are nearly zonal for these sites (compare thick and thin full lines in Fig. 6). This enhanced zonal dispersion has previously been diagnosed from float trajectories in the North Atlantic by Spall et al. (1993). However, in the Gulf Stream at 2000 m, there is strong, nearly *isotropic* dispersion where Q is nearly uniform, rather than enhanced zonal dispersion. This result suggests that Q contours are a more fundamental reference frame than geographical coordinates to understand dispersion.

The anisotropy of the dispersion is indicated by its ellipticity and the direction is measured by the angle, θ^* , made by the principle ellipse with Q (Table 4). Typically $|\theta^*|$ is less than 17° for float clusters lasting longer than 200 days and, on these longer timescales, the ratio

of the eddy dispersions along Q and across Q approaches the ellipticity of the dispersion (Table 4). For shorter timescales there are larger eddy dispersion angles for Site L and Eurofloat.

The anisotropic dispersion is not explained solely by anisotropy in the eddy velocity. In the Tropics, there are enhanced eddy velocities along Q , but in other cases the eddy velocities appear to be isotropic (including for the Eastern Basin, see Table 3). The anisotropic dispersion may instead result from eddy displacements across Q having an oscillatory nature, whereas the eddy displacements along Q increase in time following a random-walk spreading [see discussion by LaCasce and Speer (1999)].

The higher anisotropic dispersion along Q implies a higher “eddy” diffusivity acting along Q . It is unclear whether this anisotropic diffusivity reflects the action of time-varying, geostrophic eddies or results from the aliasing of small-scale, time-mean flow into these “eddy” statistics. For example, if the northern and southern Eurofloat groups are analyzed together, then the “eddy” dispersion shows enhanced dispersion along meridional Q contours. In contrast, when the Eurofloat experiment is split into two groups (as here), the “eddy” signal appears instead as a different time-mean flow for each group. However, whatever separation between *mean* and *eddy* flow is chosen, our results still suggest that passive tracers preferentially spread along Q contours in the ocean interior.

5. Conclusions

Potential vorticity has been extensively used as a theoretical tool to understand the general circulation (e.g., Rhines and Young 1982; Luyten et al. 1983). While potential vorticity has been widely diagnosed from observations (e.g., McDowell et al. 1982; Keffer 1985; O’Dwyer and Williams 1997), its distribution is usually interpreted in terms of the movement of a passive tracer, for example, in tracking the spread of mode waters (Talley and McCartney 1982). In this study, we compare potential vorticity distributions and independent float data in order to assess how well potential vorticity is conserved along trajectories and hence test the assumptions made in theoretical models.

The large-scale potential vorticity, Q , is evaluated along approximate isentropic surfaces using bottle data from the NODC climatology. The independent float data is taken from historical data and the ongoing Eurofloat experiment in the intermediate waters in the North Atlantic. Errors in our analysis originate from (i) using a Q distribution inferred from climatology rather than synoptic data; (ii) using floats spreading on level surfaces, rather than isentropic surfaces. Our results are summarized in Fig. 8, showing the mean velocity vector, the implied Peclet number, and eddy dispersion ellipses (scaled for the same length of time) for each set of float experiments.

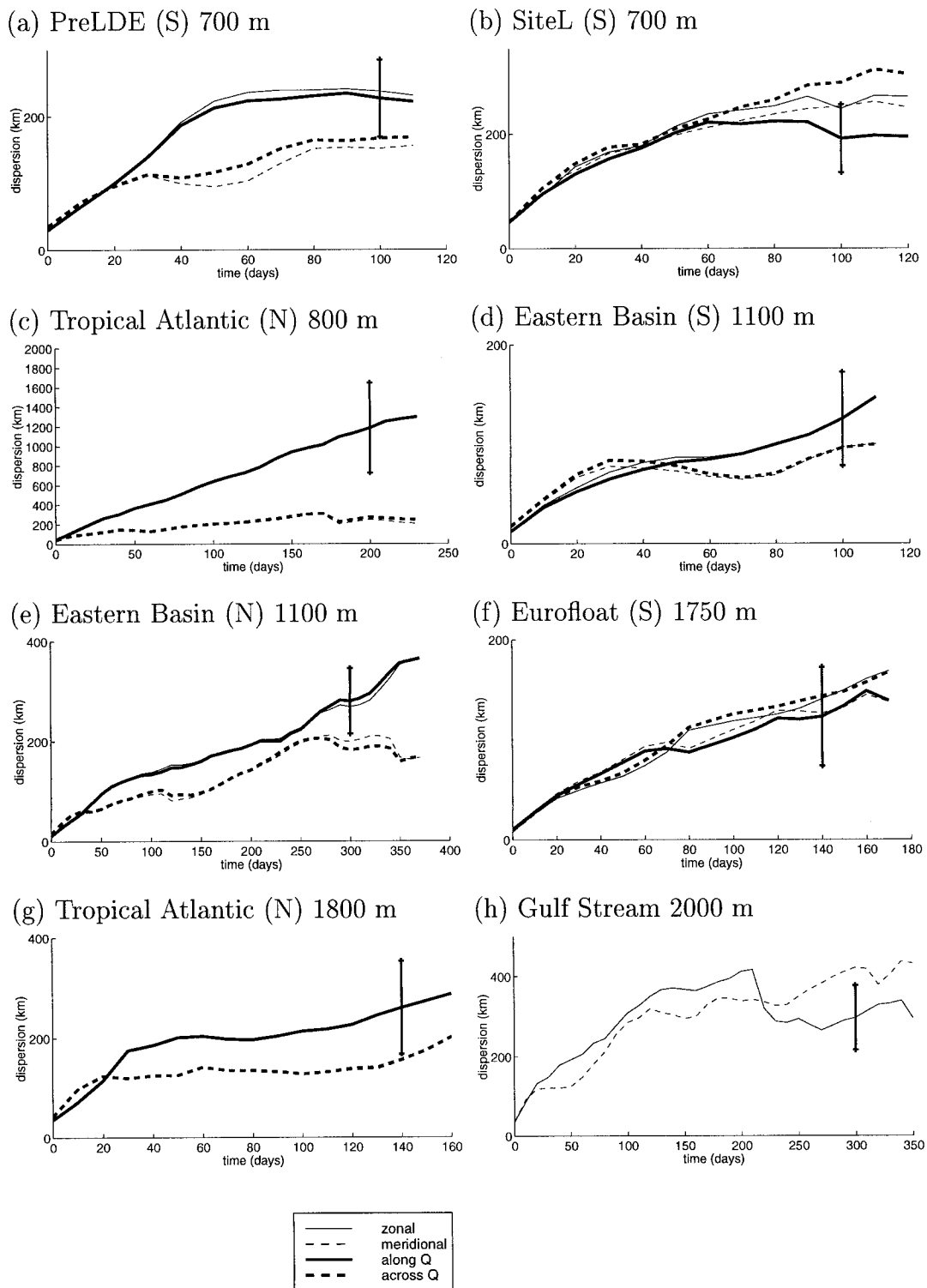


FIG. 6. Eddy dispersion of each group of floats where the time series is longer than 100 days, evaluated along Q and across Q (thick lines, respectively, solid and dashed), and for comparison zonally and meridionally (thin lines, respectively, solid and dashed). The vertical bars indicate the size of the errors. Only zonal and meridional dispersion are calculated for the Gulf Stream at 2000 m. As the number of floats decreases with time the errors in dispersion increase.

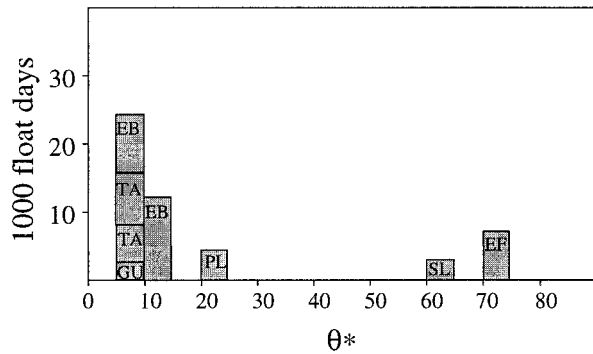


FIG. 7. Histogram of θ^* , the angle between the axis of maximum eddy dispersion and the Q contours. Boxes are labeled with the initials of the float experiments (see Table 1). The size of a box indicates the number of observations used in the analysis.

In the ocean interior, the mean velocity for the float clusters is generally greater along Q contours, than across them (see arrows in Fig. 8). This result holds even where Q contours are nearly meridional as in the Eurofloat site. Float trajectories cross Q contours at angles typically less than 20° to 30° in magnitude. The implied Peclet number, $Pe = 1/\tan\theta^*$, ranges from 1 to 19, and has a weighted mean value of 4.4, which implies that there is significant interior mixing. This value is comparable to the values 3 to 6 diagnosed in the same manner in an eddy-resolving model by Rhines and Schopp (1991) and is much smaller than the high values implied from adiabatic, inviscid thermocline models. The Peclet number reduces to less than 1 along the western boundary of the Tropics if Q contours remain zonal, which implies greater mixing and dissipation of Q ; however, this Peclet number estimate should be viewed as a lower limit, since Q contours may become aligned along the boundary current.

The Peclet number may be interpreted in terms of the

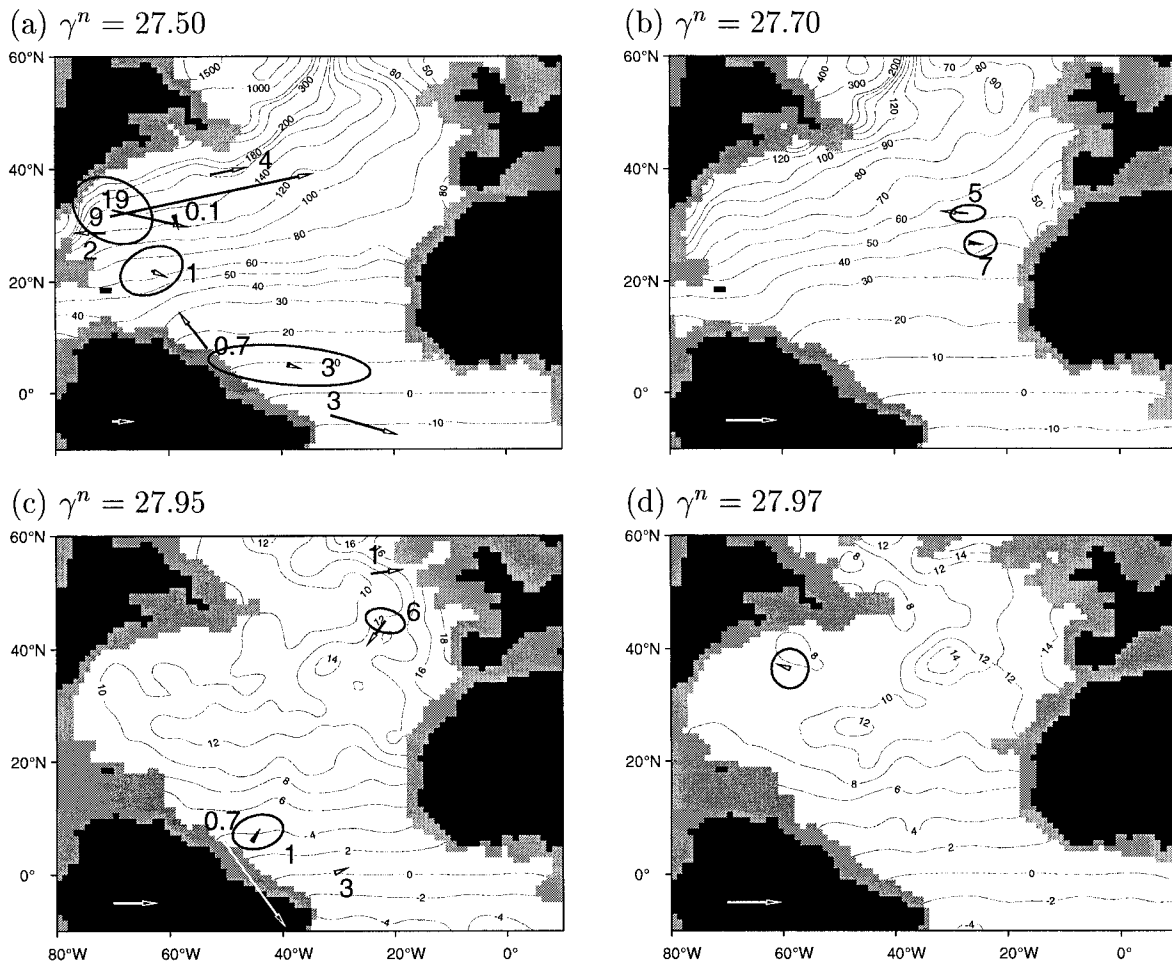


FIG. 8. A summary of float diagnostics superimposed on the corresponding Q fields. Each float experiment is labeled with its Peclet number. Mean velocities are shown by arrows [the white arrow at the bottom left is a velocity of 10 cm s^{-1} , note the different scale of (a)]. The size of the ellipse depends on the observed mean rate of dispersion extrapolated to 500 days and the orientation indicates the direction of dispersion, θ^* (Table 4). Ellipses are only shown for groups with long time series, where mean dispersion is evaluated in Table 4.

TABLE 4. Eddy dispersion for groups of floats with lifetimes longer than 100 days evaluated along and across Q contours (over the last 100 days); note some groups of floats are excluded due to insufficient data. Dispersions significantly larger along Q than across Q are underlined. The angle θ^* measures how closely the principal axis of dispersion is aligned with the direction of Q contours and the ellipticity is the ratio of the maximum to the minimum dispersion.

Experiment	Depth (m)	Length (days)	Dispersion (10^5m)		Ratio of dispersion along Q / across Q	Ellipticity	Angle $ \theta^* $ (deg)
			Along Q	Across Q			
PreLDE (S)	700	110	1.9 (± 0.4)	1.4 (± 0.3)	1.4	1.8	24
SiteL (S)	700	120	2.0 (± 0.3)	2.5 (± 0.5)	0.8	1.5	61
Gulf Stream*	2000	350	3.0 (± 0.4)	4.0 (± 0.4)	—	1.4	—
Tropical Atlantic (N)	800	230	10.8 (± 1.8)	2.6 (± 0.3)	4.2	4.4	9
Tropical Atlantic (N)	1800	160	2.3 (± 0.4)	1.5 (± 0.3)	1.5	1.7	13
Eastern Basin (N)	1100	370	3.1 (± 0.5)	1.8 (± 0.2)	1.7	1.7	11
Eastern Basin (S)	1100	110	0.9 (± 0.2)	0.8 (± 0.1)	1.1	1.2	8
Eurofloat (S)	1750	170	1.1 (± 0.2)	1.4 (± 0.2)	0.8	1.1	75

distance a tracer plume spreads along streamlines (Fig. 5). If there is a tracer contrast with a length scale L_{tracer} , then the tracer plume penetrates over a scale $L_{\text{tracer}}\text{Pe}$ before tracer contrasts are smeared out by diffusion. Our interior Peclet number of typically 4 suggests that a tracer plume with $L_{\text{tracer}} \sim 300$ km should persist for 1200 km downstream along mean streamlines. Hence, tracers should only be quasi-conserved along mean streamlines over a subbasin scale, rather than over an entire basin.

The eddy dispersion of floats also appears to be affected by the background Q distribution. Enhanced dispersion occurs along Q contours in the Tropics and eastern basin where there are long float records (see Fig. 6 and dispersion ellipses in Fig. 8). Shorter float records are ambiguous. In general, this anisotropic dispersion along Q is difficult to distinguish from enhanced zonal dispersion. However, strong *isotropic* dispersion occurs near the Gulf Stream at 2000 m where Q is nearly uniform, rather than enhanced zonal dispersion. Consequently, understanding the dispersion of floats in terms of Q coordinates appears to be more fundamental than in terms of the traditional, geographic coordinates.

In conclusion, the Q distribution appears to constrain the spreading of floats over the subbasin scale over the ocean interior, although there is significant mixing over the basin scale. The preferential spreading of floats along Q contours suggests that tracer distributions in coarse-resolution models may be improved if a larger eddy diffusion coefficient is used *along* Q contours than across them. In particular, plumes of tracer extending along Q contours may result from enhanced eddy dispersion, even in regions where the large-scale time-mean flow is weak.

Acknowledgments. JO and JL are grateful for support from the EU MAST-2 programme EUROFLOAT (PL920057), RGW for support from NERC UK WOCE Special Topic (GST/02/1686), and KS for support from CNRS.

REFERENCES

- Bower, A. S., and H. D. Hunt, 2000: Lagrangian observations of the Deep Western Boundary Current in the North Atlantic Ocean. Part II: The Gulf Stream–deep western boundary Current cross-over. *J. Phys. Oceanogr.*, in press.
- Colin de Verdiere, A., 1992: On the southward motion of Mediterranean salt lenses. *J. Phys. Oceanogr.*, **22**, 413–420.
- Davis, R. E., 1991: Observing the general circulation with floats. *Deep-Sea Res.*, **38**, S531–S571.
- Flierl, G. R., 1987: Isolated eddy models in geophysics. *Annu. Rev. Fluid Mech.*, **19**, 493–530.
- Freeland, H. J., P. B. Rhines, and T. Rossby, 1975: Statistical observations of the trajectories of neutrally buoyant floats in the North Atlantic. *J. Mar. Res.*, **33**, 383–404.
- Jackett, D. R., and T. J. McDougall, 1997: A neutral density variable for the world's oceans. *J. Phys. Oceanogr.*, **27**, 237–263.
- Jenkins, W. J., 1988: The use of anthropogenic tritium and helium-3 to study subtropical ventilation and circulation. *Philos. Trans. Roy. Soc. London*, **325A**, 43–61.
- Keffer, T., 1985: The ventilation of the world's oceans: Maps of the potential vorticity field. *J. Phys. Oceanogr.*, **15**, 509–523.
- Krauss, W., and C. W. Böning, 1987: Lagrangian properties of eddy fields in the northern North Atlantic as deduced from satellite-tracked buoys. *J. Mar. Res.*, **45**, 259–291.
- LaCasce, J. H., and K. G. Speer, 1999: Lagrangian statistics in unforced barotropic flows. *J. Mar. Res.*, **57**, 245–274.
- Levitus, S., and T. P. Boyer, 1994: *World Ocean Atlas 1994*. Vol. 4: *Temperature*, NOAA Atlas NESDIS 4, U.S. Department of Commerce, Washington, DC, 129 pp.
- , R. Burgett, and P. Boyer, 1994: *World Ocean Atlas*. Vol. 3: *Salinity*, NOAA Atlas NESDIS 3, U.S. Department of Commerce, Washington, DC, 111 pp.
- Lozier, M. S., M. McCartney, and W. B. Owens, 1994: Anomalous anomalies in averaged hydrographic data. *J. Phys. Oceanogr.*, **24**, 2624–2638.
- Luyten, J. R., J. Pedlosky, and H. Stommel, 1983: The ventilated thermocline. *J. Phys. Oceanogr.*, **13**, 292–309.
- McDowell, S., P. B. Rhines, and T. Keffer, 1982: North Atlantic potential vorticity and its relation to the general circulation. *J. Phys. Oceanogr.*, **12**, 1417–1436.
- O'Dwyer, J., and R. G. Williams, 1997: The climatological distribution of potential vorticity over the abyssal ocean. *J. Phys. Oceanogr.*, **27**, 2488–2506.
- Owens, W. B., 1991: A statistical description of the mean circulation and eddy variability in the northwestern Atlantic using SOFAR floats. *Progress in Oceanography*, Vol. 28, Pergamon, 257–303.
- Price, J. F., and W. B. Owens, 1998: Bobber trajectories from the

- Subduction Experiment. *IAPSO Proc. XXI General Assembly*, 132 pp.
- , T. K. McKee, W. B. Owens, and J. R. Valdes, 1987: Site L SOFAR float experiment, 1982–1985. Woods Hole Oceanographic Institution Tech. Rep. WHOI-87-52, 289 pp. [Available from Woods Hole Oceanographic Institution, Woods Hole, MA 02543.]
- Rhines, P. B., and W. R. Young, 1982: Homogenization of potential vorticity in planetary gyres. *J. Fluid Mech.*, **122**, 347–367.
- , and R. Schopp, 1991: The wind-driven circulation: Quasi-geostrophic simulation and theory for nonsymmetric winds. *J. Phys. Oceanogr.*, **21**, 1438–1469.
- Richardson, P. L., D. Walsh, L. Armi, M. Schroder, and J. F. Price, 1989: Tracking three meddies with SOFAR floats. *J. Phys. Oceanogr.*, **19**, 371–383.
- , M. E. Zemanovic, C. M. Wooding, and W. J. Schmitz Jr., 1994: SOFAR float trajectories in the tropical Atlantic 1989–1992. Woods Hole Oceanographic Institution Tech. Rep. WHOI-94-33, 185 pp. [Available from Woods Hole Oceanographic Institution, Woods Hole, MA 02543.]
- Robbins, P. E., J. F. Price, W. B. Owens, and W. J. Jenkins, 2000: The importance of lateral diffusion for the ventilation of the lower thermocline in the subtropical North Atlantic. *J. Phys. Oceanogr.*, **30**, 67–89.
- Spall, M. A., J. Price, and P. H. Richardson, 1993: Advection and eddy mixing in the Mediterranean salt tongue. *J. Mar. Res.*, **51**, 797–818.
- Speer, K., J. Gould, and J. LaCase, 1999: Year-long trajectories in the Labrador Sea Water of the eastern North Atlantic Ocean. *Deep-Sea Res. II*, **46**, 165–179.
- Talley, L. D., and M. S. McCartney, 1982: Distribution and circulation of Labrador Sea Water. *J. Phys. Oceanogr.*, **12**, 1189–1205.
- Zemanovich, M. E., P. L. Richardson, and J. F. Price, 1990: SOFAR float Mediterranean Outflow Experiment: Summary and data from 1986–1988. Woods Hole Oceanographic Institution Tech. Rep. WHOI-90-01, 243 pp. [Available from Woods Hole Oceanographic Institution, Woods Hole, MA 02543.]